THE JOURNAL OF BIOLOGICAL CHEMISTRY VOL. 286, NO. 8, pp. 6192–6200, February 25, 2011

A Specific Interaction of Small Molecule Entry Inhibitors with the Envelope Glycoprotein Complex of the Junín Hemorrhagic Fever Arenavirus*[S]

Received for publication, October 20, 2010, and in revised form, December 13, 2010 Published, JBC Papers in Press, December 15, 2010, DOI 10.1074/jbc.M110.196428

Celestine J. Thomas[‡§1], Hedi E. Casquilho-Gray[¶], Joanne York[¶], Dianne L. DeCamp[‡‖], Dongcheng Dai[**], Erin B. Petrilli[‡‡], Dale L. Boger[§§], Richard A. Slayden[‡‡], Sean M. Amberg[**], Stephen R. Sprang[‡§], and Jack H. Nunberg[¶2]

From the [‡]Center for Biomolecular Structure and Dynamics, [§]Division of Biological Sciences, [¶]Montana Biotechnology Center, [‖]Department of Biomedical and Pharmaceutical Sciences, University of Montana, Missoula, Montana 59812, [**]SIGA Technologies, Inc., Corvallis, Oregon 97333, the [‡‡]Department of Microbiology, Immunology, and Pathology, Colorado State University, Ft. Collins, Colorado 80523, and the [§§]Department of Chemistry, The Scripps Research Institute, La Jolla, California 92037

Arenaviruses are responsible for acute hemorrhagic fevers worldwide and are recognized to pose significant threats to public health and biodefense. Small molecule compounds have recently been discovered that inhibit arenavirus entry and protect against lethal infection in animal models. These chemically distinct inhibitors act on the tripartite envelope glycoprotein (GPC) through its unusual stable signal peptide subunit to stabilize the complex against pH-induced activation of membrane fusion in the endosome. Here, we report the production and characterization of the intact transmembrane GPC complex of Junín arenavirus and its interaction with these inhibitors. The solubilized GPC is antigenically indistinguishable from the native protein and forms a homogeneous trimer in solution. When reconstituted into a lipid bilayer, the purified complex interacts specifically with its cell-surface receptor transferrin receptor-1. We show that small molecule entry inhibitors specific to New World or Old World arenaviruses bind to the membrane-associated GPC complex in accordance with their respective species selectivities and with dissociation constants comparable with concentrations that inhibit GPC-mediated membrane fusion. Furthermore, competitive binding studies reveal that these chemically distinct inhibitors share a common binding pocket on GPC. In conjunction with previous genetic studies, these findings identify the pH-sensing interface of GPC as a highly vulnerable target for antiviral intervention. This work expands our mechanistic understanding of arenavirus entry and provides a foundation to guide the development of small molecule compounds for the treatment of arenavirus hemorrhagic fevers.

The Arenaviridae comprise a diverse group of rodent-borne viruses, some of which are associated with severe hemorrhagic fevers in humans (1). At least five species are recognized to cause fatal disease in the Americas (2, 3). Lassa fever virus (LASV)[3] is endemic in western Africa (4) and can be imported to the United States and Europe by infected travelers (5, 6). In addition, new pathogenic species continue to emerge (3, 7). In the absence of effective treatment or immunization, the hemorrhagic fever arenaviruses remain a pressing public health and biodefense concern (8, 9).

Antiviral strategies to interfere with virus entry into the host cell have in many instances proven successful in preventing virus infection and mitigating disease. Arenavirus entry takes place in the endosome through a process of pH-dependent membrane fusion, mediated by the viral envelope glycoprotein (GPC) (1). GPC is unique among class I viral fusion proteins (10, 11) in that the mature complex contains a stable signal peptide (SSP) in addition to the prototypical receptor-binding and transmembrane fusion subunits (G1 and G2, respectively) (12). Interactions between the ectodomains of SSP and G2 are thought to play a role in maintaining the prefusion form of GPC at neutral pH and activating the conformational changes leading to membrane fusion at acidic pH (13).

Independent high throughput screening (HTS) exercises at SIGA Technologies and the Scripps Research Institute (TSRI) have to date identified six chemically distinct classes of small molecule compounds that specifically inhibit GPC-mediated membrane fusion with differing selectivities against New World (NW) and/or Old World (OW) arenavirus species (Fig. 1) (14–17). Despite these chemical differences, genetic studies of antiviral resistance among the four classes of SIGA inhibitors have suggested that all these inhibitors act through the pH-sensitive interface of the SSP and G2 subunits in GPC

* This work was supported, in whole or in part, by National Institutes of Health Grants R01 AI074818 and U54 AI065357 (to J. H. N.) and P01 CA078045 (to D. L. B.). D. Dai and S. Amberg are employees of SIGA Technologies, which has interests in the compounds reported.

[S] The on-line version of this article (available at http://www.jbc.org) contains supplemental Figs. S1 and S2.

[1] Recipient of a Rocky Mountain Regional Center of Excellence for Biodefense and Emerging Infectious Diseases Research Travel award. To whom correspondence may be addressed. Tel.: 406-243-6065; Fax: 406-243-5461; E-mail: celestine.thomas@umontana.edu.

[2] To whom correspondence may be addressed. Tel.: 406-243-6421; Fax: 406-243-6425; E-mail: jack.nunberg@umontana.edu.

[3] The abbreviations used are: LASV, Lassa fever virus; JUNV, Junín virus; HTS, high throughput screening; TSRI, the Scripps Research Institute; NW and OW, New and Old World, respectively; SSP, stable signal peptide; DDM, dodecyl β-D-maltoside; icd-GPC, insect-cell derived cleavage-defective GPC; TfR1, transferrin receptor-1; sTfR, soluble transferrin receptor; DMPC, dimyristoylphosphatidylcholine; PC, phosphatidylcholine; SPR, surface plasmon resonance; NNRTI, non-nucleoside analog HIV-1 reverse transcriptase inhibitor; dansyl, 5-dimethylaminonaphthalene-1-sulfonyl; RU, response unit.

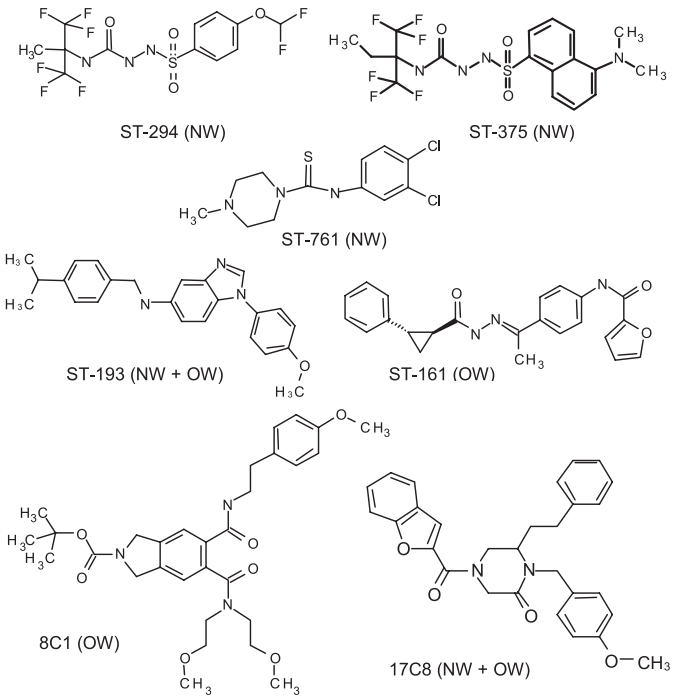

FIGURE 1. **Chemical structures of fusion inhibitors.** The *ST-* prefix identifies compounds from SIGA Technologies, and 8C1 and 17C8 are from TSRI. The inhibitory specificities for NW and/or OW arenaviruses are listed.

(14, 16, 17). Using GPC of the Junín virus (JUNV), the causative agent of Argentine hemorrhagic fever, such studies have further suggested that the inhibitors prevent virus entry by stabilizing the prefusion GPC complex against pH-induced activation in the endosome (17). One lead compound, ST-294, has also been shown to protect against lethal arenavirus infection in a small animal model (14).

Accordingly, a detailed understanding of the molecular events in membrane fusion will be important in guiding the design of optimized drug candidates for clinical development. Toward this end, we have produced the intact transmembrane JUNV GPC complex in insect cells and characterized its interaction with the chemically distinct classes of small molecule fusion inhibitors. We find that solubilized GPC forms a homogeneous trimeric complex capable of binding fusion inhibitors in an arenavirus species-specific manner. Through competitive binding studies, we also provide direct evidence that the diverse SIGA and TSRI inhibitors share a common binding pocket on GPC and likely a common mechanism of action. Biophysical and structural analysis of the bound GPC complex will provide a platform for the development of effective therapeutics for use in the treatment of arenaviral hemorrhagic fevers.

EXPERIMENTAL PROCEDURES

Monoclonal Antibodies and Small Molecule Inhibitors—Monoclonal antibodies (MAbs) directed to JUNV nucleoprotein or the G1 subunit of GPC were obtained from the Centers for Disease Control and Prevention (18) through the National Institutes of Health NIAID Biodefense and Emerging Infectious Diseases Research Resources Repository, and the anti-FLAG M2 mAb was purchased (Sigma). The small molecule fusion inhibitors discovered by SIGA Technologies, ST-761, ST-193 (16), ST-161 (17), ST-294 (14), and its dansyl analog ST-375, were obtained from the company. ST-545 (2,2′-bibenzimidazole) is an unrelated compound used as a negative control. These compounds were dissolved in dimethyl sulfoxide to a concentration of 10–50 mM and stored at −80 °C in light-resistant glass bottles. The TSRI compounds 17C8 and 8C1 (15) were originally provided by Stefan Kunz, Andrew M. Lee. and Michael B. A. Oldstone. All compounds were characterized by electrospray mass spectrometry. Chemical structures are shown in Fig. 1.

Recombinant Baculovirus Expressing Cleavage-defective JUNV GPC (icd-GPC)—Recombinant baculoviruses were generated using the Invitrogen Bac-to-Bac™ system. Coding regions corresponding to SSP and the G1G2 precursor of GPC from the pathogenic MC2 strain of JUNV (GenBank™ accession number D10072) (12, 19) were inserted downstream of the baculovirus p10 and polyhedrin protein promoters, respectively, in the pFastBac-Dual vector (Invitrogen). The G1G2 precursor was expressed using the convention signal peptide from human CD4 (12). In this mode of GPC expression, SSP and the G1G2 precursor are translated independently and associate in *trans* to reconstitute the native GPC complex (20, 21). Proteolytic maturation of the G1G2 precursor was abrogated by mutation at the SKI-1/S1P recognition site (12, 22–24), and a FLAG tag sequence was appended to the C terminus to facilitate purification. Previous studies have shown similar C-terminal tags to be innocuous (12, 25, 26). Bacmids were generated using *Escherichia coli* DH10Bac cells (Invitrogen), and these were used to transfect *Spodoptera frugiperda* Sf9 cells (Invitrogen) to generate the recombinant baculovirus.

Expression and Purification of icd-GPC—Baculoviruses encoding icd-GPC were used to infect *Trichoplusia ni* High-Five™ cells (Invitrogen) for expression and protein purification. Cultures were inoculated with the P3 virus stock at a density of 2×10^6 cells/ml and allowed to grow at 27 °C for 48–52 h. The cells were pelleted and frozen at −80 °C and subsequently thawed and resuspended in lysis buffer (25 mM Tris, 250 mM NaCl, 2 mM $MgCl_2$, 100 μM $ZnCl_2$, and protease inhibitors, pH 7.4). Nitrogen decompression (Parr Bomb) was used to disrupt cells, which were then subjected to a low speed spin to remove cellular debris. The membrane fraction was recovered by ultracentrifugation at 100,000 × *g* for 1 h. The pellet was resuspended in high salt lysis buffer containing 450 mM NaCl and again recovered by ultracentrifugation. Membranes were solubilized in lysis buffer containing 150 mM NaCl and 1.5% dodecyl β-D-maltoside (DDM) using a Dounce homogenizer. The lysate was stirred for 2 h and clarified (100,000 × *g* for 1 h), and the supernatant was incubated with M2 anti-FLAG mAb immobilized to agarose beads (Sigma) for 2 h with slight agitation. The beads were then loaded onto a column and washed with DDM-containing lysis buffer to remove nonspecifically bound proteins, and icd-GPC was eluted with 5 μM of 3×FLAG peptide (Sigma). The eluate was dialyzed to remove the peptide and subjected to size-exclusion chromatography using a Superdex-200/G-75 tandem column (GE Healthcare). All buffers included 100 μM

$ZnCl_2$ to maintain the intersubunit zinc-binding domain in GPC (27).

Gel filtration was also used to exchange detergents and vary DDM concentrations. A panel of detergents of varying hydrophobic/hydrophilic properties, lipid chain length, and head groups were investigated to optimize for retention of the trimeric state of icd-GPC. Detergents (Anatrace) included the following β-D-maltosides in addition to DDM: *n*-tridecyl-, *n*-tetradecyl-, *n*-octyl-, *n*-undecyl-, 5-cyclohexyl-1-pentyl- (Cymal-5), and 6-cyclohexyl-1-hexyl- (Cymal-6). Others tested include nonanoyl-*N*-methyl glucamide (Mega-9), decanoyl-*N*-methyl glucamide (Mega-10), *n*-octyl-β-D-glucoside, diheptanoyl phosphatidylcholine, and *n*-dodecylphosphocholine.

Biosensor Analysis in Detergent-containing Solution—The Biacore T100 system was used to analyze binding to immobilized icd-GPC. M2 anti-FLAG mAb was covalently bound to a Biacore CM5 chip by amine coupling, and 800–1500 response units (RUs) of detergent-solubilized icd-GPC were captured through the C-terminal FLAG tag. The biosensor running buffer (25 mM HEPES, 150 mM NaCl, 100 μM $ZnCl_2$, pH 7.2) contained 0.1% DDM. An unrelated membrane protein, hexahistidine aquaporin, was kindly provided by T. C. Mou (University of Montana) and captured analogously using a covalently coupled anti-hexahistidine mAb (Sigma). Multiple concentrations of mAb (0.1–2.5 μM), soluble TfR (sTfR) from human plasma (American Research Products, Inc) (0.5–5.0 μM), or small molecule compounds (5–250 μM) were injecting in matching detergent-containing buffers, and sensorgrams were recorded. After each experiment, the surface of the chip was regenerated using a pulse of glycine HCl, pH 3.0, and each surface was reused at least 20 times (or until decreased icd-GPC binding was observed).

As the RU increase associated with the binding of small molecule compounds was relatively low, several precautions were taken to enhance signal-to-noise ratios and data reliability. All experiments used similar RU levels of immobilized icd-GPC, and each small molecule concentration was repeated at least four times, and the sensorgrams were numerically averaged. Data were analyzed using Biacore kinetic analysis software and SCRUBBER, kindly provided by David G. Myszka (University of Utah). Results from both methods were concordant, and values obtained from Biacore software are reported. Final figures were generated using a five-point smoothing procedure in ORIGIN graphing software.

Preparation of Liposomes—Dimyristoylphosphatidylcholine (DMPC) and phosphatidylcholine (Avanti Polar Lipids) were used at a 4:1 molar ratio to generate liposomes, with or without the addition of 5% cholesterol hemisuccinate (Sigma). The lipids, dissolved in chloroform, were mixed and thoroughly dried to the bottom of a round-bottomed flask. Multilamellar vesicles were formed in vesicle buffer (20 mM Tris, 150 mM NaCl, 1 mM EDTA, pH 8.5) with vigorous vortexing in the presence of glass beads. After removal of the glass beads, vesicles were subjected to six cycles of freeze-thaw and extruded through polycarbonate filters (100-nm pores; Aventis). Liposomes were diluted 1:50 into biosensor running buffer (without detergent) and used immediately for binding to a Biacore L1 chip (see below) or snap-frozen in liquid nitrogen. Frozen samples required additional extrusion through a polycarbonate filter (100 nm) prior to use.

Biosensor Analysis of Lipid-reconstituted icd-GPC—icd-GPC was immobilized and reconstituted into a lipid bilayer on a Biacore L1 chip using minor modifications of the procedure described by Myszka and co-workers (28). Briefly, M2 anti-FLAG mAb was covalently coupled to the L1 chip, and the surface was briefly rinsed with 20 mM CHAPS detergent (Sigma). icd-GPC was subsequently bound in detergent-containing biosensor running buffer to an appropriate RU level. DMPC-phosphatidylcholine liposomes diluted into detergent-free running buffer were then introduced in an extended injection (40 min at 5 μl/min) to allow liposome binding to the lipophilic surface of the L1 chip, where they subsequently coalesce to form a lipid bilayer and displace protein-bound detergent. The surface was then washed until a stable base line was obtained, whereupon the binding of MAbs, sTfR, and small molecule compounds was analyzed as described above. The L1 chip was regenerated with a 1-min pulse of isopropyl alcohol, 40 mM NaOH (2:3 v/v) at 30 μl/min to remove lipids and associated proteins. The anti-FLAG mAb was reconditioned with a pulse of glycine HCl, pH 3.0, and washed extensively with running buffer prior to reuse. For kinetic calculations, all the plasma-derived soluble transferrin receptor was assumed to be TfR1.

Fluorescence Assays—Dansyl ST-375 (10 μM) was incubated with 1 μM icd-GPC in assay buffer (25 mM Tris, 150 mM NaCl, 100 μM $ZnCl_2$, 0.1% DDM, and protease inhibitors, pH 7.4), and binding was followed by an increase in dansyl fluorescence as a function of time. Samples were excited at 340 nm, and the dansyl emission was measured at 525 nm in an L55 luminometer (PerkinElmer Life Sciences) equipped with a circulating water bath maintained at 20 °C. To assess competitive binding, the ST-375·icd-GPC complex was formed by incubation for 2 h at 4 °C, and unbound ST-375 was subsequently removed by ultrafiltration (Amicon). The complex was readjusted to 1 μM, and nonfluorescent inhibitor was added to 10 μM. Dissociation of ST-375 was measured by the decrease in dansyl fluorescence as a function of time. ST-294·icd-GPC complexes were similarly prepared to examine effects on ST-375 binding.

Characterization of GPC in Mammalian Cells—Wild-type and cleavage defective GPC were expressed in Vero cells by *trans*-complementation as described previously (12, 19). Briefly, two pcDNA3.1-based plasmids (Invitrogen) containing the bacteriophage T7 promoter and encoding, respectively, SSP and the G1G2 precursor were co-transfected into Vero cells infected with the vTF7-3 recombinant vaccinia virus expressing T7 RNA polymerase (29). For immunoprecipitation studies, cells expressing cleavage defective-GPC were metabolically labeled from 6 to 16–24 h post-transfection using 50 μCi/ml ^{35}S-ProMix (GE Healthcare) and cultures were subsequently harvested in buffer containing 1% Triton X-100 (12, 19). Similar immunoprecipitation studies were conducted using metabolically labeled High-Five™ insect cells expressing icd-GPC.

Inhibition of GPC-mediated membrane fusion by small molecule compounds was assessed using a vaccinia virus-based β-galactosidase fusion-reporter assay (30) as described previously (12, 13). Vero cells expressing GPC (and the T7 polymerase) were co-cultured with target cells infected with the vCB21R-lacZ vaccinia virus bearing the β-galactosidase gene under the control of a T7 promoter (30). Cell-cell fusion was initiated by briefly exposing the co-culture to medium adjusted to pH 5.0 and reported by expression of β-galactosidase 5 h after return to neutral pH. β-Galactosidase activity was quantified using the chemiluminescent GalactoLite Plus substrate (Applied Biosystems) and a Tropix TR717 microplate luminometer. In inhibition studies, co-cultures were incubated with serial dilutions of the compounds for 3 h prior to exposure to pH 5.0 (17). EC_{50} values (concentrations at which inhibition is at 50%) were calculated using relative light units normalized to the no-inhibitor control value and a three-variable nonlinear best fit algorithm in Prism software (GraphPad).

RESULTS

Expression of Cleavage-defective JUNV GPC—Recombinant baculoviruses provide a robust platform for high level expression of membrane glycoproteins (31); thus we proceeded to express the intact transmembrane GPC complex of JUNV in insect cells. In constructing the recombinant baculovirus, we took advantage of the observation from mammalian cells that SSP can be translated independently and will associate in *trans* with the G1G2 precursor to reconstitute the native GPC complex (20, 21). This strategy obviates reported inefficiencies in signal peptidase cleavage of the nascent GPC polypeptide and potentially confounding effects of mutations in SSP (12, 32). Thus, a baculovirus pFastBac-Dual (Invitrogen) vector was used to express SSP separately from the G1G2 precursor, which was directed to the membrane by the conventional signal peptide of human CD4 (12) and included a C-terminal FLAG tag sequence to facilitate purification. As in other class I viral fusion proteins (10, 11, 33), the G1G2 precursor must be cleaved to generate the mature G1 and G2 subunits and actuate the membrane fusion potential of the complex. This cleavage, however, is generally incomplete on overexpression of recombinant protein. To obtain a homogeneous protein product, we mutated the SKI-1/S1P recognition site to prevent cleavage (12). Other studies have suggested that a lack of cleavage may also enhance the structural stability of envelope complexes during purification (34). The icd-GPC was isolated from membranes of High-Five™ cells by solubilization in buffer containing 1.5% DDM. Affinity purification using the C-terminal FLAG tag resulted in co-isolation of the untagged SSP subunit (Fig. 2, *inset*), demonstrating association with the G1G2 precursor as described in mammalian cells (20, 21). The yield of purified icd-GPC by this procedure was ~1 mg/liter of High-Five™ cell culture.

Size-exclusion chromatography demonstrated that icd-GPC exists in solution as a relatively homogeneous complex of ~220 kDa (Fig. 2), consistent with a GPC trimer and with the trimeric organization of other class I virus fusion proteins (reviewed in Refs. 35–37). The stability of the trimeric structure was highly dependent on the nonionic detergent used; glucosidal detergents tended to induce formation of higher order multimers, whereas the trimer was retained in maltoside (including DDM) and Cymal detergents. Fos-choline and its relatives induced precipitation of the protein. In suitable detergents (*e.g.* DDM), the icd-GPC trimer was stable for several weeks at 4 °C.

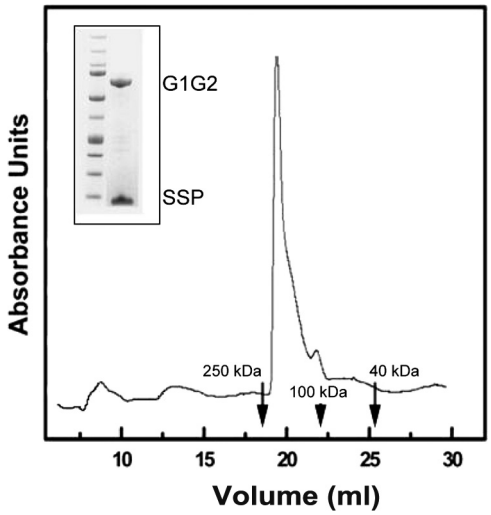

FIGURE 2. **Purification of icd-GPC.** The icd-GPC protein was purified from insect cell membranes using a FLAG tag and subjected to gel filtration on a tandem G200/G75 matrix in detergent-containing buffer. Absorbance is monitored at 280 nm, and molecular size standards are indicated by *arrows*. The gel filtration profile indicates that the detergent-bound icd-GPC elutes as a trimer of ~220 kDa. The *inset* shows a Coomassie-stained SDS-polyacrylamide gel to demonstrate the purity of the complex and the presence of SSP, with molecular size standards shown on the *left*. The Precision Blue (Bio-Rad) proteins indicate 250, 150, 100, 75, 50, 37, 25, 20, 15, and 10 kDa, from top to bottom.

icd-GPC Is Antigenically Similar to Native GPC—To assess whether icd-GPC folds into a native conformation, we performed immunoprecipitation studies using a panel of five well characterized G1-directed MAbs raised against γ-ray-irradiated JUNV virions (18). Four of these MAbs (BE08, AG02, BF11, and AA09) are capable of neutralizing viral infectivity (18) and would serve as sensitive probes for the native GPC conformation. As illustrated in supplemental Fig. S1, all five G1-directed MAbs were able to immunoprecipitate icd-GPC, with efficiencies comparable with those seen with mammalian cell-derived cleavage-defective GPC. GPC was not precipitated by a control mAb (BG12) directed to the JUNV nucleoprotein (18). These studies indicate that icd-GPC is antigenically similar to the native GPC complex.

To obtain a quantitative assessment of mAb recognition, icd-GPC was immobilized onto a CM5 biosensor chip, and binding was detected by surface plasmon resonance (SPR) using a Biacore T100 instrument. icd-GPC was captured by its C-terminal FLAG tag using an anti-FLAG antibody covalently coupled to the biosensor chip. The collection of sensorgrams acquired at different mAb concentrations was used to determine kinetic parameters and dissociation constants (Table 1). Representative sensorgrams are shown in supplemental Fig. S2. As anticipated from immunoprecipitation studies, all five G1-directed MAbs showed strong binding to the immobilized icd-GPC. K_d values ranged from 11 to 900 nM. The rank order

TABLE 1

Summary of interaction parameters determined from surface-plasmon resonance studies

NB means no binding detected.

	Detergent			Lipid-reconstituted		
	k_a	k_d	K_d	k_a	k_d	K_d
	$M^{-1}s^{-1}$	s^{-1}	nM	$M^{-1}s^{-1}$	s^{-1}	nM
MAb						
BF11	5.3×10^5	0.006	11.3	5.9×10^5	0.006	10.1
BF09	2.1×10^5	0.06	285.7	3.2×10^5	0.07	218.7
AA09	5.2×10^5	0.08	150.8	5.6×10^5	0.07	125.0
BE08	1.6×10^5	0.07	437.5	1.2×10^5	0.07	538.3
AG02	8.9×10^4	0.08	898.8	8.1×10^4	0.08	987.6
AB11			NB			NB
BG12			NB			NB
sTfR			NB	5.4×10^{-4}	0.07	1296.3
	k_a	k_d	K_d	k_a	k_d	K_d
	$M^{-1}s^{-1}$	s^{-1}	μM	$M^{-1}s^{-1}$	s^{-1}	μM
Compounds						
ST-294	6.4×10^3	0.08	12.5	9.2×10^3	0.01	1.08
ST-193	1.1×10^3	0.09	76.8	1.9×10^3	0.02	10.52
ST-761	1.3×10^3	0.09	69.2	2.3×10^3	0.02	8.67
ST-375	2.5×10^3	0.08	23.5	2.9×10^3	0.01	3.45
ST-161			NB			NB
ST-545			NB			NB
17C8	3.4×10^3	0.09	26.4	4.2×10^3	0.04	9.50
8C1			NB			NB

of these values is not predictive of virus neutralization activity (18), as the non-neutralizing mAb BF09 (280 nM) bound with higher affinity than the neutralizing MAbs BE08 (440 nM) and AG02 (900 nM).

JUNV entry is initiated by GPC binding to transferrin receptor-1 (TfR1) on the cell surface (38). We thus examined the ability of the detergent-solubilized icd-GPC to bind to plasma-derived soluble transferrin receptor (sTfR; American Research Products), a preparation that contains both TfR1 and TfR2. Only TfR1 is used for virus entry (38). No binding was detected under these conditions (supplemental Fig. S2).

Membrane-reconstituted icd-GPC Binds sTfR—The viral GPC is anchored in the membrane through the transmembrane domain of G2 and the two hydrophobic regions of SSP (39). Despite the apparent stability of the detergent-bound icd-GPC complex, insertion within a lipid bilayer environment might impart a more native-like structure to the trimeric complex. To investigate this notion, we reconstituted solubilized icd-GPC into a lipid membrane on the surface of an L1 biosensor chip (28). icd-GPC was immobilized as described above, but in this study the detergent was replaced by liposomes containing DMPC and phosphatidylcholine, which anneal onto the lipophilic L1 chip to form a lipid bilayer that accommodates the transmembrane domain of the immobilized protein (28). The reconstituted complex generated a stable SPR base line upon washing in detergent-free buffer and thus provided a suitable substrate to assess binding. Reconstitution of icd-GPC in membrane did not alter recognition by the G1-directed MAbs (Table 1), yet it had a dramatic effect on the binding of sTfR (Fig. 3). An analysis of concentration-dependent sensorgrams indicated that sTfR bound the membrane-reconstituted icd-GPC with a K_d of ~1.3 μM (Table 1). sTfR did not bind to surfaces devoid of icd-GPC or to lipid bilayers containing the unrelated membrane protein aquaporin.

The K_d value for sTfR binding to membrane-associated icd-GPC is consistent with that determined by J. Abraham and H. Choe (Harvard Medical School),[4] using recombinant G1 from the closely related Machupo virus and a soluble truncated form of TfR1 (40). The apparent requirement for lipid in our studies may indicate stabilization of the icd-GPC com-

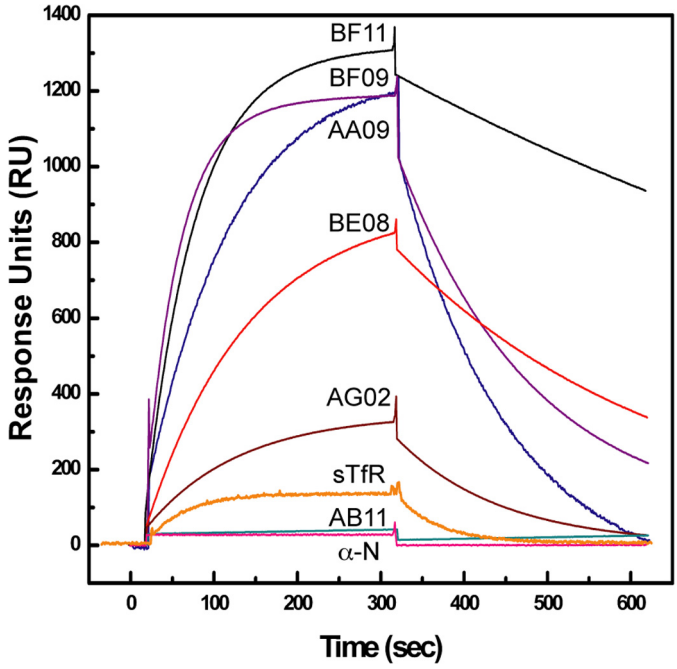

FIGURE 3. **Biosensor analysis of the interaction of MAbs and sTfR with membrane-associated icd-GPC.** The icd-GPC complex was immobilized on an L1 chip and DMPC:phosphatidylcholine liposomes were used to generate a lipid bilayer. Concentration-dependent sensorgrams were analyzed, and representative interactions with JUNV-specific MAbs (18) and soluble TfR from human plasma (American Research Products) are shown. MAbs were injected at a concentration of 500 nM. mAb BF11 (*black*), BF09 (*purple*), AA09 (*blue*), BE08 (*red*), and AG02 (*wine*) are directed to JUNV G1. BG12 (*cyan*) recognizes JUNV N protein (α-*N*) and the protein target of AB11 (*pink*) is unknown. sTfR (*orange*) was used at 1.5 μM.

[4] J. Abraham and H. Choe, personal communication.

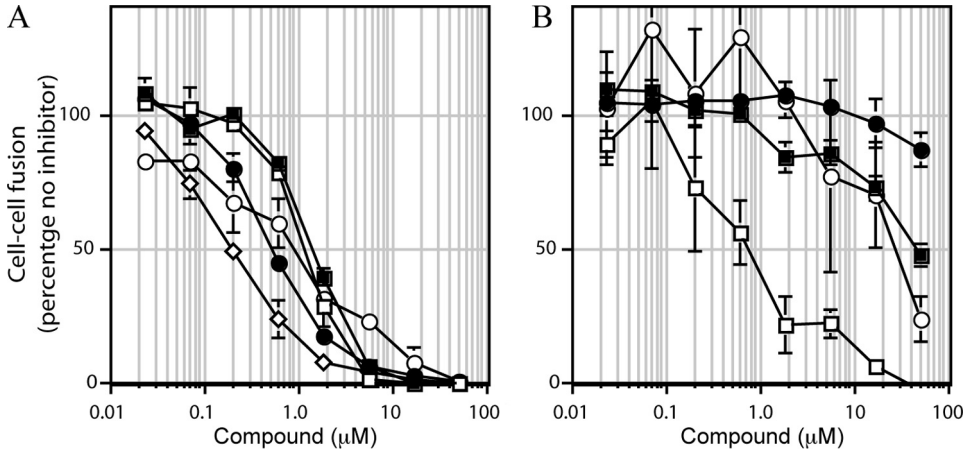

FIGURE 4. **Inhibition of pH-induced cell-cell fusion.** The inhibitory potency of SIGA and TSRI compounds was determined as described previously using a vaccinia virus-based β-galactosidase fusion-reporter assay (12, 13, 30). Serial dilutions of test compounds were added for 3 h prior to the induction of cell-cell fusion by exposure to medium adjusted to pH 5.0. Inhibition is plotted as a percentage of fusion in the absence of inhibitor. *A,* ST-761 (*open squares*), ST-193 (*open circles*), ST-375 (*closed circles*), and 17C8 (*open diamonds*). *B,* inhibition of wild-type (*filled symbols*) and K33H (*open symbols*) GPC using the OW-specific inhibitors ST-161 (*circles*) and 8C1 (*squares*). 8C1 displays weak activity against wild-type JUNV GPC, and the K33H mutation increases susceptibility to both compounds. *Error bars* represent one S.D. among replicates and may not be visible on the scale of the graph; those in studies using K33H GPC are relatively large because of the lower fusion activity of this mutant. EC_{50} values reported in the text were calculated using the three-variable nonlinear best fit algorithm of Prism software (GraphPad).

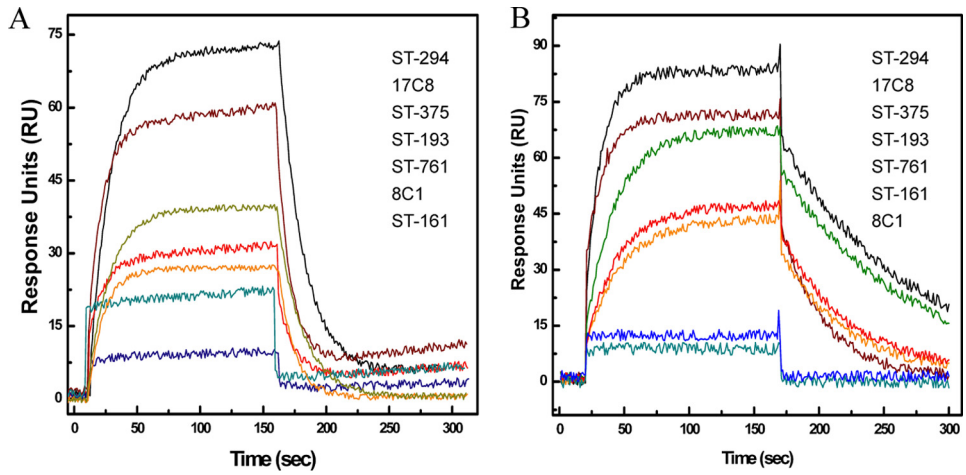

FIGURE 5. **Biosensor analysis of the interaction of small molecule fusion inhibitors with icd-GPC.** *A,* icd-GPC was immobilized on a CM5 chip in 0.1% DDM, and interactions with small molecule compounds were analyzed. Representative sensorgrams for the indicated SIGA and TSRI compounds (used at 150 and 100 μM, respectively) are shown. Inhibitors are listed in the order corresponding to their final RU value in the association phase and are indicated by color as follows: ST-294 (*black*), 17C8 (*wine*), ST-375 (*olive*), ST-193 (*red*), ST-761 (*orange*), ST-161 (*purple*), and 8C1 (*cyan*). *B,* icd-GPC complex was reconstituted into lipid bilayer on an L1 chip, and interactions with small molecule compounds were analyzed as above. Representative sensorgrams are shown.

plex, but it is also possible that the sTfR ligand itself is sensitive to nonionic detergent. The biologically relevant binding of native membrane-anchored GPC to cell-associated TfR1 has not been examined in detail.

icd-GPC Binds Small Molecule Fusion Inhibitors—As icd-GPC retains many of the essential structural features of the native GPC complex, we wanted to determine whether the recombinant protein might serve as a platform for physicochemical studies of small molecule fusion inhibitors. To date, six distinct chemical classes of inhibitors (Fig. 1) have been identified through independent HTS programs at SIGA Technologies and TSRI. Among these, ST-294 and ST-761 are specific to the NW arenaviruses, and ST-193 and TSRI 17C8 inhibit both NW and OW viruses (Fig. 4*A*) (14–16). Therefore, these compounds might be expected to bind JUNV GPC *in vitro*. By contrast, ST-161 and TSRI 8C1 are selective for the OW LASV (Fig. 4*B*) (15, 17). Binding of these compounds to icd-GPC was initially examined using a CM5 biosensor chip in detergent-containing solution. As illustrated in representative sensorgrams (Fig. 5*A*), all compounds capable of inhibiting JUNV GPC-mediated membrane fusion bound to icd-GPC. No binding was observed using chip surfaces devoid of icd-GPC or those containing the unrelated membrane protein aquaporin. Binding was also abolished in the presence of non-maltoside detergents that disrupt the trimeric structure of the complex. Importantly, the LASV-specific inhibitors ST-161 and 8C1 did not bind to JUNV icd-GPC. Together, these studies validate the specificity and sensitivity of the biosensor measurements of inhibitor binding. We conclude that species selectivity among these diverse inhibitors is determined by GPC binding, rather than through post-binding effects.

Membrane Reconstitution Enhances Binding to Approximate Fusion-inhibitory Concentrations—To investigate inhibitor binding under more native conditions, we made use of

membrane-reconstituted icd-GPC on an L1 biosensor chip (see above). As shown in Fig. 5*B*, species-specific binding of the inhibitors was retained upon membrane insertion of icd-GPC. Importantly, the binding affinities to membrane-associated icd-GPC were enhanced on average 8-fold relative to those obtained using the detergent-solubilized complex (Table 1). These increases bring the calculated K_d values (1.1–10.5 μM) closer to the EC_{50} values obtained for inhibition of cell-cell fusion in culture (Fig. 4*A*, 0.2–1.5 μM). For ST-294, the K_d and EC_{50} values were equal. Among the other SIGA compounds, the K_d and EC_{50} values differed by at most 10-fold. For 17C8, the discrepancy was ~50-fold. We also observed only minimal correlations with EC_{50} values among the active compounds, suggesting that interactions beyond simple affinity may also contribute to potency.

We note that the decrease in K_d values on membrane reconstitution is largely attributable to decreases in the dissociation rates (k_d). Although it is possible that the decrease in K_d values simply reflects more favorable partitioning of the hydrophobic compounds to the protein in the absence of detergent, this effect might be expected to alter both k_a and k_d values. The specific decrease in k_d suggests rather that membrane insertion stabilizes the icd-GPC complex.

Our results also indicate that the fusion inhibitors bind to GPC containing the uncleaved G1G2 precursor, as well as to the mature fusion-competent complex. We propose that uncleaved icd-GPC bears important structural similarities to the mature prefusion GPC complex, and we speculate that conformational changes induced upon proteolytic maturation of the G1G2 precursor may be localized and limited, as reported for the influenza hemagglutinin (HA) (41).

SIGA and TSRI Inhibitors Share a Common Binding Site—ST-375 (Fig. 1) is a dansyl analog of ST-294 that inhibits JUNV GPC-mediated cell-cell fusion at an EC_{50} similar to that of its parent (Fig. 4*A*, 0.6 and 1.5 μM for ST-375 and ST-294, respectively). As the fluorescent properties of dansyl compounds are often sensitive to chemical environment, and specifically to protein binding (42), we asked if we could detect ST-375 binding to icd-GPC as a change in dansyl fluorescence emission. ST-375 fluorescence at 525 nm did indeed increase in a time-dependent manner on binding to solubilized icd-GPC (Fig. 6, *inset*). This increase was somewhat delayed when ST-375 was added to preformed ST-294·icd-GPC complex (Fig. 6, *inset*) and was unaffected by the addition of the unrelated molecule ST-545. By contrast, no change in fluorescence emission was observed in the absence of icd-GPC or on incubation of ST-375 with the unrelated membrane protein aquaporin (Fig. 6, *inset*). Together, these data validate the use of dansyl fluorescence to assess ST-375 binding to icd-GPC in solution.

This then allowed us to determine whether any of the chemically distinct fusion inhibitors might compete with ST-375 for binding, as had been suggested based on genetic studies of cross-resistance among the SIGA compounds (16, 17). Consistent with the notion that these inhibitors share a common binding site, we found that ST-375 could be displaced from icd-GPC by ST-294 in a time- and concentration-dependent manner (Fig. 6). Bound ST-375 was also displaced by

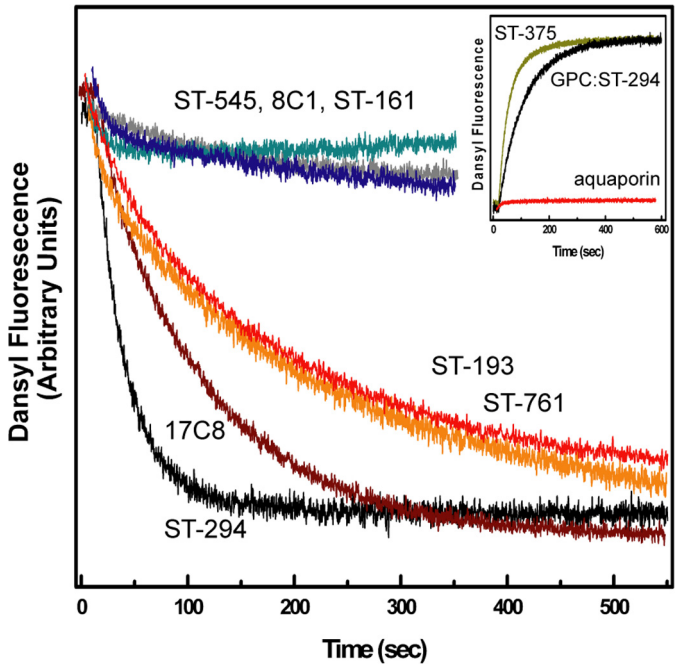

FIGURE 6. **Competitive binding of small molecule fusion inhibitors to icd-GPC.** Solubilized icd-GPC was preincubated with an excess of ST-375 (a dansyl analog of ST-294) in buffer containing 0.1% DDM and rapidly desalted prior to mixing with a 10-fold excess of nonfluorescent compound (10 μM). The loss in fluorescence at 525 nm due to displacement of ST-375 by the following compounds was monitored: ST-294 (*black*), 17C8 (*wine*), ST-761 (*orange*), ST-193 (*red*), ST-161 (*blue*), 8C1 (*cyan*), and an unrelated compound ST-545 (*gray*) failed to displace ST-375. The *inset* demonstrates the time-dependent gain in fluorescence on initial ST-375 binding (*olive*). Binding is delayed on incubation with preformed ST-294·icd-GPC complex (*black*) and absent if the unrelated membrane protein aquaporin (*red*) is substituted for icd-GPC.

ST-761 and ST-193 but not by the LASV-specific inhibitor ST-161. Despite its independent provenance, the broadly active TSRI inhibitor 17C8 was also able to displace ST-375 from icd-GPC, whereas the LASV-specific compound 8C1 did not (Fig. 6). Together, these results corroborate the specificity of the competitive binding assay and the hypothesis that the chemically distinct JUNV inhibitors share a common binding site.

Although we cannot formally exclude the alternative possibility that ST-375 is displaced through allosteric effects of binding at a second site on GPC, the central role of SSP in determining sensitivity to multiple classes of inhibitors argues instead for a shared binding site at the SSP-G2 interface (14, 16, 17). For instance, we have shown that the K33H mutant of JUNV GPC is resistant to ST-294 yet exhibits *de novo* sensitivity to the LASV-specific inhibitor ST-161 (17). Similarly, K33H JUNV GPC is also hypersensitive to 8C1 (Fig. 4*B*). From these observations, we infer that ST-161 and 8C1 bind the homologous SSP-G2 interface on LASV GPC. All the independently derived SIGA and TSRI arenavirus entry inhibitors are thus directed to a common molecular target on GPC.

DISCUSSION

Small molecule inhibitors of GPC-mediated virus entry show early promise toward the development of effective therapies to treat the often fatal hemorrhagic fevers. To understand the molecular basis by which these small molecule com-

pounds act to inhibit pH-dependent activation of membrane fusion by GPC, we have purified and characterized the intact transmembrane envelope glycoprotein of JUNV. The recombinant icd-GPC complex is produced from insect cells in milligram quantities and captures many of the essential features of the native viral protein. The purified complex includes SSP and assembles as a trimer, a hallmark of class I viral fusion proteins. The complex is antigenically indistinguishable from the native protein and, upon reconstitution into a lipid bilayer, is able to bind the cellular receptor for the virus, TfR1. In addition, the recombinant protein binds small molecule fusion inhibitors in accordance with their selectivities for NW and OW arenaviruses. Taken together, our results suggest that icd-GPC represents a native conformational state of the viral protein.

Viral envelope glycoprotein complexes are inherently labile, poised to undergo a series of conformational changes leading to formation of a thermodynamically favored postfusion structure (reviewed in Refs. 35–37). Activation of this process is controlled by cell-surface receptors or access to specific intracellular compartments to ensure productive entry of the viral genome. The labile prefusion state, which is established on proteolytic maturation of the envelope glycoprotein precursor, is maintained in part by insertion of the complex in the membrane. In the absence of cleavage, the precursor complex is more stable yet also shows a propensity to form heterogeneous oligomers and postfusion-like structures on solubilization (34). The inherent lability of class I envelope glycoproteins has limited efforts to define prefusion structures and has frustrated efforts to produce native complexes for effective immunization (43). The apparent stability of the GPC trimer is likely due in part to the lack of proteolytic cleavage in the icd-GPC mutant but may also be facilitated by interactions among nine membrane-spanning domains (compared with three in conventional class I fusion proteins).

Genetic and antiviral resistance studies have suggested that the inhibitory effect of the SIGA compounds is mediated through the pH-sensitive interaction between the SSP and G2 ectodomains (17). The TSRI inhibitors likely act similarly. In the case of influenza HA, the prototype pH-dependent class I virus fusion protein, the pH-sensing domain is thought to lie proximal to the fusion peptide at the interface of the HA1 and HA2 subunits (44, 45). Interestingly, several groups have described small molecule HA fusion inhibitors (TBHQ and 4c) that target this pH-sensitive interaction to stabilize the prefusion HA complex (46–48). Our findings, in a distant virus family and unique class I fusion protein, suggest that localized intersubunit interactions associated with activation of membrane fusion may present vulnerable targets for antiviral intervention against other pathogenic viruses that utilize the class I fusion mechanism.

Identification of a common binding pocket and mechanism-of-action among the small molecule arenavirus fusion inhibitors brings to mind the well studied example of the nonnucleoside analog HIV-1 reverse transcriptase inhibitors (NNRTIs). These chemically distinct compounds bind a common hydrophobic pocket near the active site of RT to allosterically inhibit polymerization (49, 50). The NNRTI-binding site is not directly associated with any known function of RT but forms a fortuitous target identified in HTS for inhibition of function. On binding to RT, these compounds adopt a "butterfly-like" shape, and structural knowledge of this binding pocket has successfully guided the design of second and third generation NNRTIs (51). In contrast to HIV-1 RT and influenza HA, atomic level structural information of the fusion inhibitor-bound GPC complex is not yet available. In its absence, it may be possible to discern spatial and chemical commonalities among these chemically diverse yet functionally similar molecules using computational methods (52). Nonetheless, the information gleaned from quantitative analysis of GPC binding can provide a valuable complement in guiding the development of optimized compounds for clinical study in the treatment of arenavirus hemorrhagic fevers.

Acknowledgments—We are grateful to Dr. Ragavan Swaminathan (University of Texas Southwestern Medical Center) for performing pilot biosensor experiments. We thank Dr. David G. Myszka (University of Utah) for providing SCRUBBER software and Dr. Tung Chung Mou (University of Montana) for the kind gift of purified aquaporin and for helpful discussions during icd-GPC purifications. J. H. N. thanks Drs. Stefan Kunz, Andrew Lee, and Michael Oldstone for initially providing TSRI fusion inhibitors, and C. J. T. acknowledges Erika Gustafson for assistance in tissue culture maintenance. Monoclonal antibodies directed to JUNV N and GPC were obtained from the National Institutes of Health Biodefense and Emerging Infections Research Resources Repository. Biosensor studies were performed at the Rocky Mountain Regional Center of Excellence for Biodefense and Emerging Infectious Diseases Research and Proteomics Core at Colorado State University.

REFERENCES

1. Buchmeier, M. J., de la Torre, J. C., and Peters, C. J. (2007) in *Fields Virology* (Knipe, D. M., and Howley, P. M., eds) 5th Ed., pp. 1791–1828, Lippincott Williams & Wilkins, Philadelphia
2. Peters, C. J. (2002) *Curr. Top. Microbiol. Immunol.* **262,** 65–74
3. Delgado, S., Erickson, B. R., Agudo, R., Blair, P. J., Vallejo, E., Albariño, C. G., Vargas, J., Comer, J. A., Rollin, P. E., Ksiazek, T. G., Olson, J. G., and Nichol, S. T. (2008) *PLoS Pathog.* **4,** e1000047
4. McCormick, J. B., Webb, P. A., Krebs, J. W., Johnson, K. M., and Smith, E. S. (1987) *J. Infect. Dis.* **155,** 437–444
5. Haas, W. H., Breuer, T., Pfaff, G., Schmitz, H., Köhler, P., Asper, M., Emmerich, P., Drosten, C., Gölnitz, U., Fleischer, K., and Günther, S. (2003) *Clin. Infect. Dis.* **36,** 1254–1258
6. Amorosa, V., MacNeil, A., McConnell, R., Patel, A., Dillon, K. E., Hamilton, K., Erickson, B. R., Campbell, S., Knust, B., Cannon, D., Miller, D., Manning, C., Rollin, P. E., and Nichol, S. T. (2010) *Emerg. Infect. Dis.* **16,** 1598–1600
7. Palacios, G., Savji, N., Hui, J., Travassos da Rosa, A., Popov, V., Briese, T., Tesh, R., and Lipkin, W. I. (2010) *J. Gen. Virol.* **91,** 1315–1324
8. Department of Health and Human Services (2007) *Federal Register* **72,** 20117–20128
9. NIAID (2011) *NIAID Category A, B, and C Priority Pathogens,* http://www.niaid.nih.gov/topics/BiodefenseRelated/Biodefense/research/Pages/CatA.aspx
10. Eschli, B., Quirin, K., Wepf, A., Weber, J., Zinkernagel, R., and Hengartner, H. (2006) *J. Virol.* **80,** 5897–5907
11. York, J., Berry, J. D., Ströher, U., Li, Q., Feldmann, H., Lu, M., Trahey, M., and Nunberg, J. H. (2010) *J. Virol.* **84,** 6119–6129
12. York, J., Romanowski, V., Lu, M., and Nunberg, J. H. (2004) *J. Virol.* **78,** 10783–10792

13. York, J., and Nunberg, J. H. (2006) *J. Virol.* **80,** 7775–7780
14. Bolken, T. C., Laquerre, S., Zhang, Y., Bailey, T. R., Pevear, D. C., Kickner, S. S., Sperzel, L. E., Jones, K. F., Warren, T. K., Amanda Lund, S., Kirkwood-Watts, D. L., King, D. S., Shurtleff, A. C., Guttieri, M. C., Deng, Y., Bleam, M., and Hruby, D. E. (2006) *Antiviral Res.* **69,** 86–97
15. Lee, A. M., Rojek, J. M., Spiropoulou, C. F., Gundersen, A. T., Jin, W., Shaginian, A., York, J., Nunberg, J. H., Boger, D. L., Oldstone, M. B., and Kunz, S. (2008) *J. Biol. Chem.* **283,** 18734–18742
16. Larson, R. A., Dai, D., Hosack, V. T., Tan, Y., Bolken, T. C., Hruby, D. E., and Amberg, S. M. (2008) *J. Virol.* **82,** 10768–10775
17. York, J., Dai, D., Amberg, S. M., and Nunberg, J. H. (2008) *J. Virol.* **82,** 10932–10939
18. Sanchez, A., Pifat, D. Y., Kenyon, R. H., Peters, C. J., McCormick, J. B., and Kiley, M. P. (1989) *J. Gen. Virol.* **70,** 1125–1132
19. York, J., and Nunberg, J. H. (2009) *J. Virol.* **83,** 4121–4126
20. Eichler, R., Lenz, O., Strecker, T., Eickmann, M., Klenk, H. D., and Garten, W. (2003) *EMBO Rep.* **4,** 1084–1088
21. Agnihothram, S. S., York, J., and Nunberg, J. H. (2006) *J. Virol.* **80,** 5189–5198
22. Lenz, O., ter Meulen, J., Klenk, H. D., Seidah, N. G., and Garten, W. (2001) *Proc. Natl. Acad. Sci. U.S.A.* **98,** 12701–12705
23. Beyer, W. R., Pöpplau, D., Garten, W., von Laer, D., and Lenz, O. (2003) *J. Virol.* **77,** 2866–2872
24. Rojek, J. M., Lee, A. M., Nguyen, N., Spiropoulou, C. F., and Kunz, S. (2008) *J. Virol.* **82,** 6045–6051
25. Beyer, W. R., Miletic, H., Ostertag, W., and von Laer, D. (2001) *J. Virol.* **75,** 1061–1064
26. Capul, A. A., Perez, M., Burke, E., Kunz, S., Buchmeier, M. J., and de la Torre, J. C. (2007) *J. Virol.* **81,** 9451–9460
27. Briknarová, K., Thomas, C. J., York, J., and Nunberg, J. H. (2010) *J. Biol. Chem.* **286,** 1528–1536
28. Stenlund, P., Babcock, G. J., Sodroski, J., and Myszka, D. G. (2003) *Anal. Biochem.* **316,** 243–250
29. Fuerst, T. R., Niles, E. G., Studier, F. W., and Moss, B. (1986) *Proc. Natl. Acad. Sci. U.S.A.* **83,** 8122–8126
30. Nussbaum, O., Broder, C. C., and Berger, E. A. (1994) *J. Virol.* **68,** 5411–5422
31. Matsuura, Y., Possee, R. D., Overton, H. A., and Bishop, D. H. (1987) *J. Gen. Virol.* **68,** 1233–1250
32. Froeschke, M., Basler, M., Groettrup, M., and Dobberstein, B. (2003) *J. Biol. Chem.* **278,** 41914–41920
33. York, J., Agnihothram, S. S., Romanowski, V., and Nunberg, J. H. (2005) *Virology* **343,** 267–274
34. Earl, P. L., Doms, R. W., and Moss, B. (1990) *Proc. Natl. Acad. Sci. U.S.A.* **87,** 648–652
35. Skehel, J. J., and Wiley, D. C. (2000) *Annu. Rev. Biochem.* **69,** 531–569
36. White, J. M., Delos, S. E., Brecher, M., and Schornberg, K. (2008) *Crit. Rev. Biochem. Mol. Biol.* **43,** 189–219
37. Harrison, S. C. (2008) *Nat. Struct. Mol. Biol.* **15,** 690–698
38. Radoshitzky, S. R., Kuhn, J. H., Spiropoulou, C. F., Albariño, C. G., Nguyen, D. P., Salazar-Bravo, J., Dorfman, T., Lee, A. S., Wang, E., Ross, S. R., Choe, H., and Farzan, M. (2008) *Proc. Natl. Acad. Sci. U.S.A.* **105,** 2664–2669
39. Agnihothram, S. S., York, J., Trahey, M., and Nunberg, J. H. (2007) *J. Virol.* **81,** 4331–4337
40. Abraham, J., Corbett, K. D., Farzan, M., Choe, H., and Harrison, S. C. (2010) *Nat. Struct. Mol. Biol.* **17,** 438–444
41. Chen, J., Lee, K. H., Steinhauer, D. A., Stevens, D. J., Skehel, J. J., and Wiley, D. C. (1998) *Cell* **95,** 409–417
42. Thomas, C. J., Gangadhar, B. P., Namitha, S., and Surolia, A. (1998) *J. Am. Chem. Soc.* **120,** 12428–12434
43. Pantophlet, R., and Burton, D. R. (2006) *Annu. Rev. Immunol.* **24,** 739–769
44. Thoennes, S., Li, Z. N., Lee, B. J., Langley, W. A., Skehel, J. J., Russell, R. J., and Steinhauer, D. A. (2008) *Virology* **370,** 403–414
45. Reed, M. L., Yen, H. L., DuBois, R. M., Bridges, O. A., Salomon, R., Webster, R. G., and Russell, C. J. (2009) *J. Virol.* **83,** 3568–3580
46. Hoffman, L. R., Kuntz, I. D., and White, J. M. (1997) *J. Virol.* **71,** 8808–8820
47. Russell, R. J., Kerry, P. S., Stevens, D. J., Steinhauer, D. A., Martin, S. R., Gamblin, S. J., and Skehel, J. J. (2008) *Proc. Natl. Acad. Sci. U.S.A.* **105,** 17736–17741
48. Vanderlinden, E., Göktas, F., Cesur, Z., Froeyen, M., Reed, M. L., Russell, C. J., Cesur, N., and Naesens, L. (2010) *J. Virol.* **84,** 4277–4288
49. Esnouf, R., Ren, J., Ross, C., Jones, Y., Stammers, D., and Stuart, D. (1995) *Nat. Struct. Biol.* **2,** 303–308
50. De Clercq, E. (2004) *Chem. Biodivers.* **1,** 44–64
51. Jorgensen, W. L., Ruiz-Caro, J., Tirado-Rives, J., Basavapathruni, A., Anderson, K. S., and Hamilton, A. D. (2006) *Bioorg. Med. Chem. Lett.* **16,** 663–667
52. Martin, Y. C. (1998) in *Designing Bioactive Molecules, Three-dimensional Techniques and Applications* (Martin, Y. C., and Willett, A., eds) pp. 121–148, American Chemical Society, Washington, D.C.